bioengineering

MDPI

Article

Dynamic Foam Characteristics during Cultivation of *Arthrospira platensis*

Ameer Ali Kubar [1,2,†], Amjad Ali [3,†], Santosh Kumar [2], Shuhao Huo [1,*], Muhammad Wajid Ullah [4], Khulood Fahad Saud Alabbosh [5], Muhammad Ikram [6] and Jun Cheng [2,*]

1 School of Food and Biological Engineering, Jiangsu University, Zhenjiang 212013, China; ameerali.kubar@yahoo.com
2 State Key Laboratory of Clean Energy Utilization, Zhejiang University, Hangzhou 310027, China; santoshmalhi@zju.edu.cn
3 Research School of Polymeric Materials, School of Materials Science and Engineering, Jiangsu University, Zhenjiang 212013, China; amjadali@zju.edu.cn
4 Biofuels Institute, School of the Environment and Safety Engineering, Jiangsu University, Zhenjiang 212013, China; wajid_kundi@ujs.edu.cn
5 Department of Biology, College of Science, University of Hail, Hail 55476, Saudi Arabia; k.alabosh@uoh.edu.sa
6 Department of Pharmacy, COMSATS University Islamabad, Abbottabad Campus, Abbottabad 22060, Pakistan; ikram@cuiatd.edu.pk
* Correspondence: huo@ujs.edu.cn (S.H.); juncheng@zju.edu.cn (J.C.)
† These authors contributed equally to this work.

Abstract: This study is aimed at understanding the serious foaming problems during microalgal cultivation in industrial raceway ponds by studying the dynamic foam properties in *Arthrospira platensis* cultivation. *A. platensis* was cultivated in a 4 L bowl bioreactor for 4 days, during which the foam height above the algal solution increased from 0 to 30 mm with a bubble diameter of 1.8 mm, and biomass yield reached 1.5 g/L. The algal solution surface tension decreased from 55 to 45 mN/m, which favored the adsorption of microalgae on the bubble to generate more stable foams. This resulted in increased foam stability (FS) from 1 to 10 s, foam capacity (FC) from 0.3 to 1.2, foam expansion (FE) from 15 to 43, and foam maximum density (FMD) from 0.02 to 0.07. These results show a decrease in CO_2 flow rate and operation temperature when using the Foamscan instrument, which minimized the foaming phenomenon in algal solutions to a significantly lower and acceptable level.

Keywords: foam; stability; flow rate; photobioreactor; carbon dioxide; temperature

Citation: Kubar, A.A.; Ali, A.; Kumar, S.; Huo, S.; Ullah, M.W.; Alabbosh, K.F.S.; Ikram, M.; Cheng, J. Dynamic Foam Characteristics during Cultivation of *Arthrospira platensis*. *Bioengineering* **2022**, *9*, 257. https://doi.org/10.3390/bioengineering9060257

Academic Editors: Giorgos Markou and Imene Chentir

Received: 8 May 2022
Accepted: 9 June 2022
Published: 16 June 2022

1. Introduction

Microalgae have been the subject of growing industrial research for years due to their greater photosynthetic efficiency in utilizing CO_2, sunlight, and inorganic nutrients, which in turn contribute to reducing the effects of global warming [1,2]. Many studies have indicated that microalgae are an important source of high-value products and a strong candidate for sustainable and eco-friendly energy sources worldwide; this brings the potential to meet the need of rapidly growing economies, particularly in developing countries, by offering fewer adverse atmospheric effects [3–7]. The microalgal raceway ponds are usually 15 to 25 cm deep, supplied with a source of CO_2, equipped with a paddle wheel, and have guided barriers in the flow channel to ensure homogeneity. These raceway ponds are generally lit by sunlight under controlled temperature and have a ready source of water; this is currently the most industrially marketable technology because of its lower costs compared to the closed bioreactors [8–13].

Foaming is desirable for a number of global industries, such as in the food industry, where foam is of great importance for basic food textures owing to its lightness and large specific surface area [14–16]. Several engineering processes, however, are directly

affected by the unwanted foams, such as in metal industries, wastewater treatment plants, and anaerobic digesters. Foams can obstruct gas transport and render the process inefficient, thus significantly increasing cost [17–20]. Foam becomes problematic during algal cultivation when it is formed to a level that can hinder the regular process tasks. This phenomenon has remained unnoticed and been ignored for decades. Foams may last for short times (up to hours) on solution surfaces during large-scale algal cultivation in an open pond, as shown in Figure 1. This results in adverse effects, such as a decrease in growth, loss of volume, lower light penetration (since phototrophic microalgal cultivation strongly depends on light energy), pond structure failure, and difficult manual cleaning of the reactor. Such impacts can lead to economic losses of varying magnitudes. Numerous studies have provided advances in structural engineering in reactor design for attaining maximum algal biomass yield; however, the formation of foam during algal cultivation in photo-bioreactors is still unreported in the existing literature [21–24].

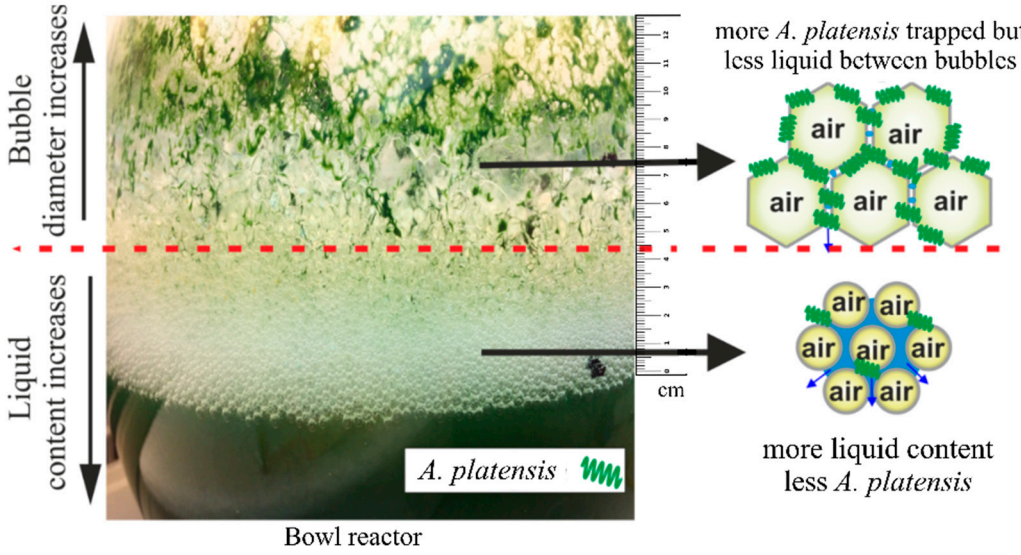

Figure 1. Formation of stable CO_2 bubbles at different foam heights.

To understand the serious foaming problems that present during microalgal cultivation in industrial raceway ponds, the dynamic foam properties from *A. platensis* cultivation were characterized in this study to clarify the processes in foam formation and foam evolution. The reduced surface tension of algal cultures, combined with ionic sulfate and phosphate surfactant adsorption on bubble walls, was found to generate more stable foams. This resulted in an increase in foam stability, foam capacity, foam expansion, and foam maximum density.

2. Materials and Methods

2.1. Instrumental Setup

The main instrument used in this study was a Foamscan system (Teclis Instruments, Civrieux-d'Azergues, France). A schematic diagram of the Foamscan instrument is shown in Figure 2. This system is connected with software for precise determination of foam volume, liquid fraction and volume, and controlling the gas flow rate, stirring speed, and measuring the bubble size and distribution. Foamscan optically measures the foaming capabilities by providing information on stability, drainage rate, and bubble size distribution [25]. Additionally, the foam column is layered with a temperature sensor inside the tube. In the present study, the Foamscan system was used to determine the foam stability (FS), foam capacity (FC), foam expansion (FE), and foam maximum density (FMD).

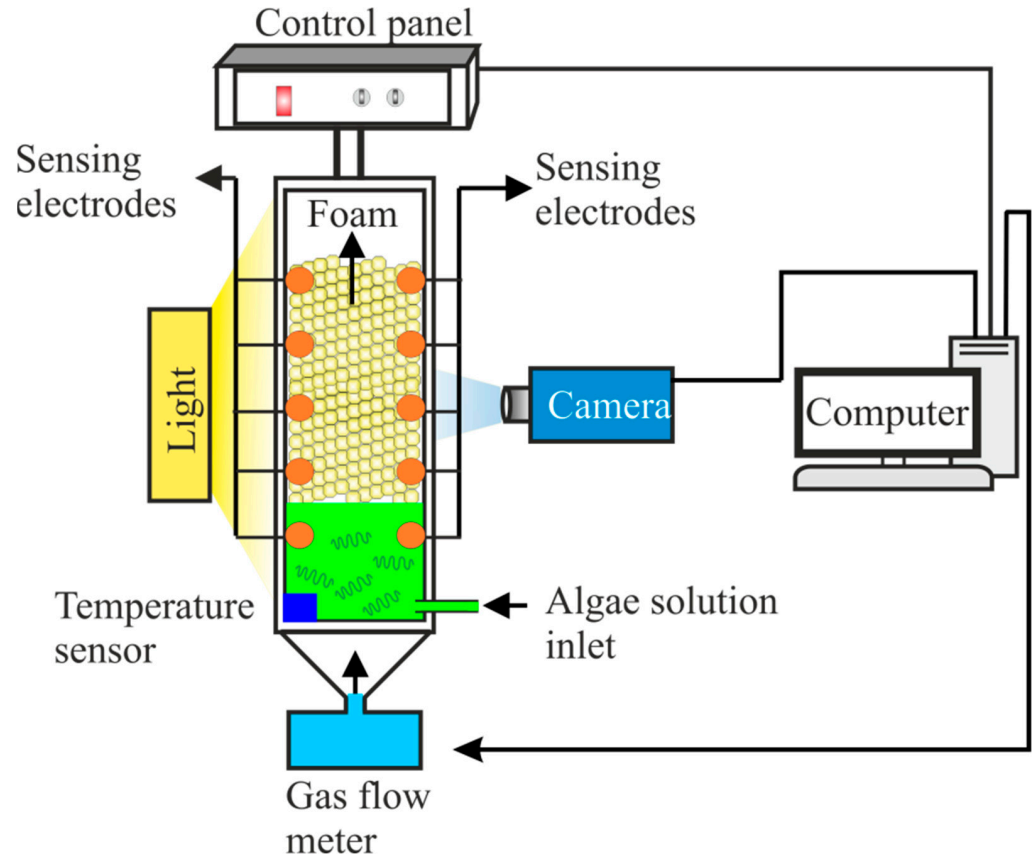

Figure 2. Schematic illustration of foam measurement system.

2.2. Foam Generation and Stability Analysis

For foam generation, a 50 mL sample solution was injected through an inlet into the foam column, equipped with a temperature sensor inside the tube. The experimental parameters were set by using the connected software. For all experiments, the final foam volume limit was set at 70 mL. The foam was generated by sparging CO_2 gas into the injected sample solution in the foam column, and its volume was controlled with the help of the connected software. Gas sparging was automatically stopped once the foam volume reached the preset final limit, and tests were performed to separately investigate the effects of CO_2 and temperature. For CO_2 flow rate tests, the temperature was fixed at 30 °C, whereas CO_2 aeration was varied according to the testing parameters (200, 250, 300, 350, and 400 mL/min). The temperature effect was determined at varying temperatures (20, 25, 30, 35, and 40 °C), whereas the CO_2 aeration rate was fixed at 300 mL/min. The foam stability, also known as the half-life, was determined in terms of FE, FC, and FMD, as described below:

FE was determined as the ratio of the total foam volume to the liquid volume within the bubbles after foam generation is completed by using Equation (1).

$$FE = \frac{Vf_{foam}}{Vi_{liq} - Vf_{liq}} \quad (1)$$

where Vf_{foam} (mL) is the total foam volume after the completion of the foaming process, Vi_{liq} (mL) is the liquid volume at the initial state, and Vf_{liq} (mL) is the volume of liquid remaining after the completion of the foaming process.

FC was determined as the ratio of the total foam volume to the gas volume after foam generation is completed by using Equation (2) [26].

$$FC = \frac{Vf_{foam}}{Vf_{gas}} \quad (2)$$

FMD was determined as the ratio of the difference between the initial liquid volume and the final liquid volume with the final foam volume.

2.3. Surface Tension

The surface tension (mN/m) of the solution was measured by using a digital surface pressure device via the du Noüy ring method. Briefly, the fluid samples were added to a container with an automated adjustable height. After each reading, the ring was thoroughly washed with double distilled water and then heated in a flame. Measurements were performed three times for reproducibility and accuracy.

2.4. Cultivation Conditions

The *A. platensis* strain was cultivated with 4 L Zarrouk's medium in a bowl photobioreactor aerated with the 15% CO_2, and the flow rate was controlled at 300 mL/min using a mass flow meter (Sevenstar CS200, Beijing, China). The experiment was conducted in an artificial climate greenhouse with an indoor temperature of 30 ± 2 °C, and the light intensity was kept at 8000 ± 200 lux. Biomass was measured using optical density with algal solution (10 mL) using a WFJ 7200 visible spectrophotometer at the wavelength of 560 nm with deionized water as blank. Error bars shown were found with Excel's standard deviation (SD) function. The pH value throughout the study was determined using an FE20 laboratory pH meter. The data for the dry weight curve of the *A. platensis* was obtained by (y = 0.51x − 0.034, where y refers to dry weight, and x refers to OD). Each measurement during all experiments was performed twice a day at 9:00 and 21:00 to ensure reproductively and accuracy of the results, and each data throughout the figures is a mean of three data with an error bar to represent uncertainty in the measurements [26].

2.5. Microscopic Observation

The bubble diameter of foam was determined, as described previously [22], by using a Nikon inverted fluorescence microscope (Nikon Corporation, Tokyo, Japan) and calculated by using software (NIS-Elements BR4.00.12). The bubble diameter was measured twice per day for 4 consecutive days. Data were collected from at least 50 bubbles each time.

3. Results and Discussion

3.1. Foam Morphology during A. platensis Cultivation

The foam morphology above the solution was observed during algal cultivation. With increasing microalgae density in solution, the surface tension decreased, which weakened the interfacial properties at the air-liquid interface. Therefore, the microalgal solution resulted in fast adsorption kinetics and high surface visco-elastic interface properties. These properties are favorable for foam formation [15,27,28]. Figure 3 illustrates the process involved in stable and unstable bubble formation and a typical mechanism of foam formation during the cultivation of *A. platensis*. A sticky gel-like material was continuously excreted through the walls of *A. platensis*, known as extracellular polymeric substance (EPS), that generated an aggregate formation by adhesion between microalgae surfaces which were trapped in the thin bubble films that promoted stable foam over the solution surface [27,28].

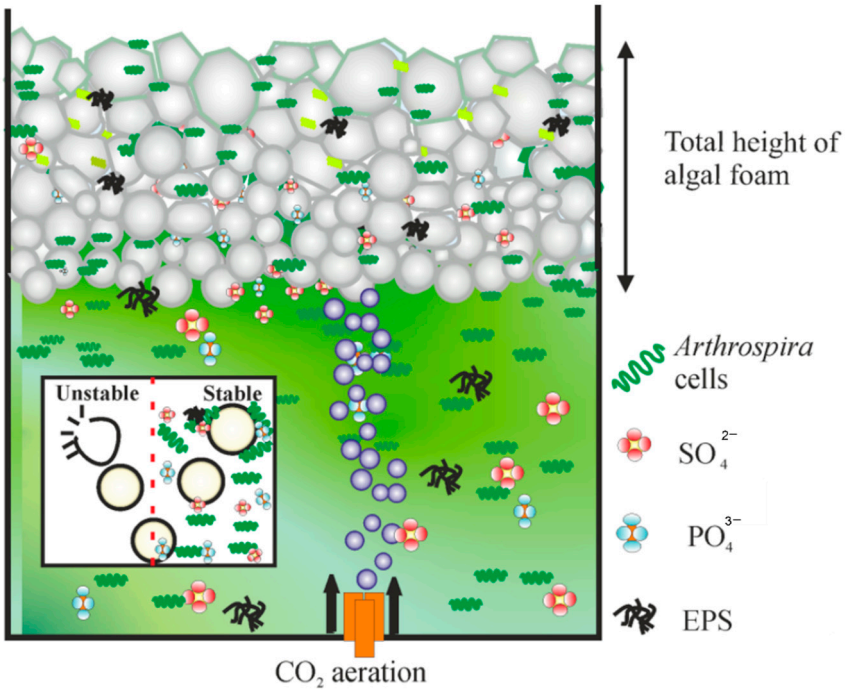

Figure 3. Mechanism of foam formation during cultivation of *A. platensis*.

As shown in Figure 4a, the foam height over the surface of microalgae solution gradually increased and reached the highest value of 30 mm after 4 days (Figure 4b). During this time, the bubble diameter also increased and reached 1.8 mm after 4 days (Figure 4b). Importantly, the bubble diameter close to the surface was smaller as compared to the bubbles located at the top of foams and away from the solution. This phenomenon occurred due to coarsening.

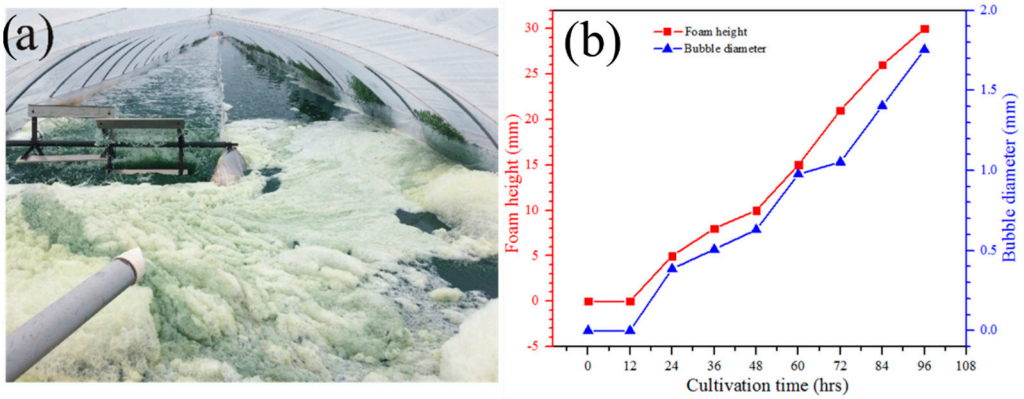

Figure 4. (**a**) Foam formation during cultivation of *A. platensis* cultivation in industrial raceway ponds (**b**) Qualitative and quantitative demonstration of increasing foam height and bubble diameter after 4 days of microalgal growth.

Bubbles generated by aeration can resist bursting because adsorption of the sticky nature of algal cells attached to bubbles led to the formation of a resistant armor that slowed down the drainage, reduced bubble breakage, and increased coarsening, which resulted in more stable and long-lasting foam [29]. As the foam height rises, bubble diameter increases, and bubbles coarsen from smaller bubbles to larger bubbles over time due to gas diffusion [30]. According to the Laplace–Young law, 'coarsening' involves the transport of gas between bubbles due to their differences in pressure, leading to an increase in the average bubble diameter over time [31,32].

3.2. Stability of Foam during Biomass Production

Foaming was a gradual and continuous process during the cultivation of microalgae, and 1.5 g/L of microalgal biomass was produced after 4 days (Figure 5). When the biomass grew denser and *A. platensis* cells started to produce EPS around their walls, a large portion of EPS was attached to the surface of *A. platensis* cells, whereas some were released into the culture medium. The separation of EPS from the cell surface is a well-established phenomenon [30,33,34]. The released EPS formed stable thin films in the solution and resulted in the formation of stable foams. This polymeric substance, i.e., EPS, consists of sulfated substitutes (0.5–22%), uronic acids (14–40%), and polysaccharides. The results showed an association between the microalgal biomass and surface tension. The surface tension continuously decreased with increasing microalgal biomass (Figure 5). The amphiphilic nature of the algal solution is due to the presence of uronic acids and peptides in EPS [35]. Therefore, the emulsifying property of the solution was significantly enhanced, which is caused by the presence of rhamnose and fucose deoxy sugars [29,33,36]. During the cultivation time, the pH of the solution also increased, although only slightly, from ~9.8 to ~10.2 (Figure 5). This slight increase in pH during foam formation could be due to the CO_2 uptake.

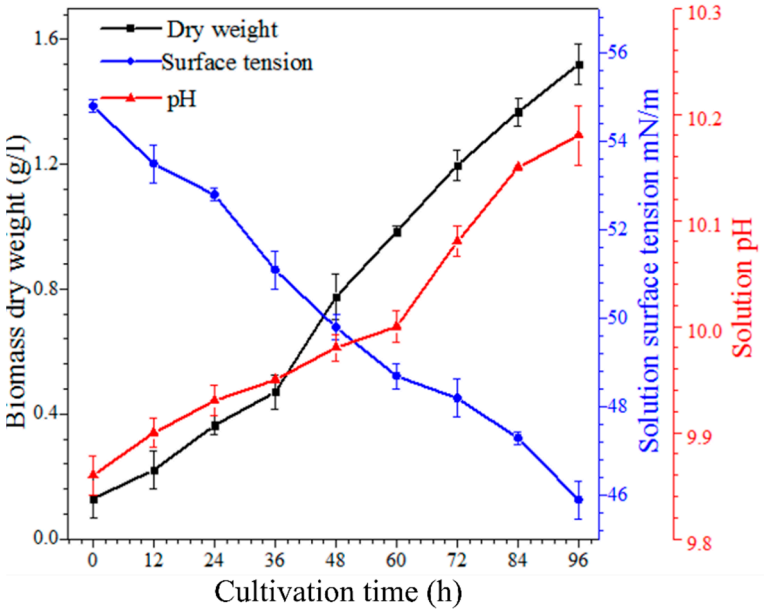

Figure 5. Formation of microalgal biomass and its impact on the solution surface tension and pH during the 4 days growth of *A. platensis*. The algal biomass increased with time, which increased the pH and decreased the surface tension of the solution.

The dependence of foaming characteristics, including FS, FC, FE, and FMD, on the microalgal growth rate was monitored (Figure 6). FC increased steadily with increasing dry biomass weight and reached 1.2 when 1.5 g/L dry biomass was produced after 4 days. A similar trend was found for FE that increased from 15 to 43 when dry biomass of 1.5 g/L was produced after 4 days. The foam produced by 1.5 g/L microalgal dry biomass remained stable for 10 s. Similarly, the FMD was increased from 0.02 to 0.07 during the formation of 1.5 g/L microalgal dry biomass. The results showed that all foaming characteristics, including FS, FC, FE, and FMD, were increased with the increasing microalgal biomass dry weight. Bubble interfaces were accumulated by microalgae together with EPS and formed a soft adhesive gel that favoured the formation of stable and long-lasting foams, as shown in Figure 4. As the microalgal density increased, the cells were adsorbed by the bubble and carried over to the surface of the solution during aeration or paddle wheel rotation. The EPS excretion gradually decreased the surface tension of the solution because

EPS behaved as a surfactant and increased the stickiness of the culture, therefore creating a positive environment to generate stable foaming [33,37].

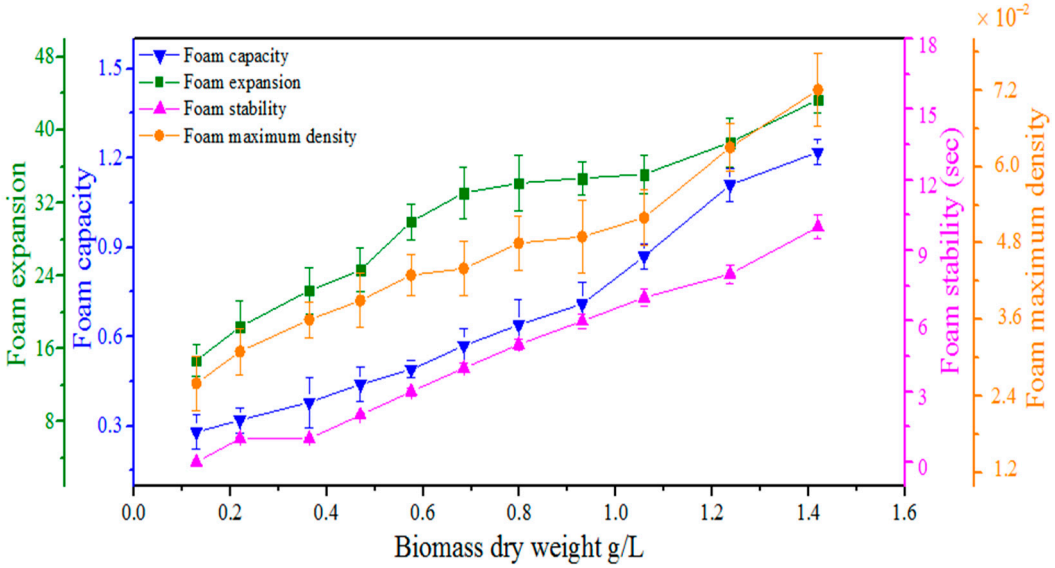

Figure 6. The dependence of foaming characteristics, including foam capacity, foam expansion, foam stability, and foam maximum density, on the microalgal biomass dry weight produced for 4 days. Note: **Foam Stability** = Half-life of foam from generation to disappear, **Foam capacity** = Ratio of foam volume to gas volume, **Foam expansion** = Ratio of foam volume to reduced liquid volume from initial to final condition, and **Foam maximum density** = Ratio of the difference between the initial liquid volume and the final liquid volume with the final foam volume. Note: Each data point is an average of three replicates with a standard deviation, $n = 3$.

3.3. Effect of CO_2 Aeration on Foam Stability

Since CO_2 gas influenced the rapid volume expansion of foam when the bioreactor was continuously aerated from the bottom, the EPS attached to the *A. platensis* cell wall enhanced the formation of stable foams. The maximum solubility of CO_2 in an algal solution was essential for efficient algal growth, but when the aeration rate became greater than the solubility capability of the solution, the supplied gas went through the algal solution idly and contributed to the foam formation on the surface of the solution.

The effect of CO_2 flow rate on the formation of foam was investigated by using the Foamscan instrument that helped to analyze four different characteristics of the algal foam, including the FS, FC, FE, and FMD. Figure 7a shows that the FS of the solution increased gradually from 1 to 10 s during the 4 days as the algal growth increased. It also showed that FC and FE increased from 0.26 ± 0.03 to 0.90 ± 0.03 and 22 ± 0.46 to 38 ± 0.46 over time (Figure 7a,b). These results indicate that CO_2 aeration and *A. platensis* cell density increased simultaneously. FMD was the only parameter that decreased from 5.5 ± 2.8 to $3.1 \times 10^{-2} \pm 2.8$ with the increasing aeration rate of gas (Figure 7b). This could be attributed to the continuous supply of CO_2 gas that led to rapid bubble formation that ruptured more quickly due to the high aeration rate. Thus, larger bubbles with lower density were formed at higher flow rates.

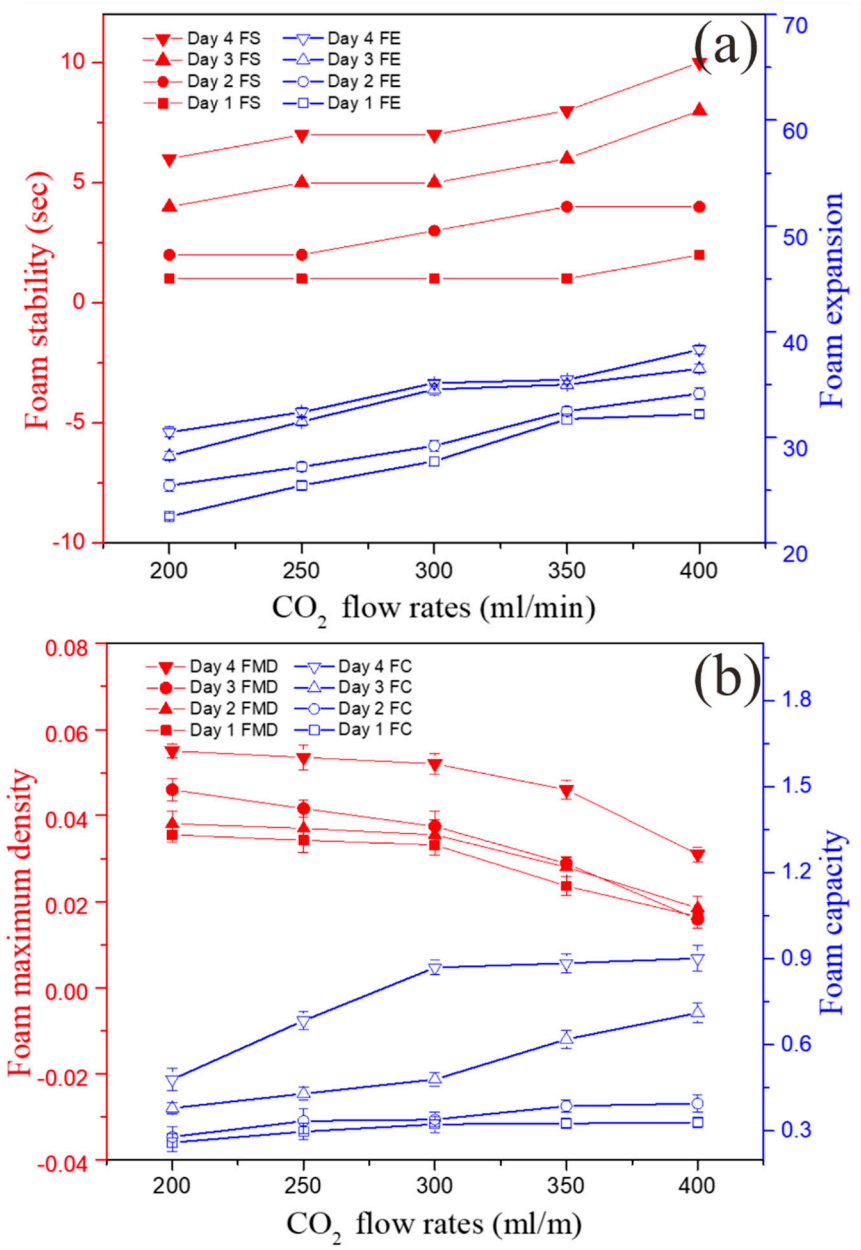

Figure 7. Effects of CO_2 flow rates on dynamic characteristics: (**a**) foam stability and expansion and (**b**) foam maximum density and capacity.

3.4. Effect of Cultivation Temperature on Foaming Stability

Temperature is one of the most important control parameters during the algal growth, as the metabolic and enzymatic activities are directly influenced by it during the simultaneous production of biomass and EPS [34,36,38]. A higher temperature reduces the solubility of gaseous components (i.e., CO_2) in the culture medium, whereas a lower temperature leads to reduced algal growth and decreases the kinetics of metabolic activities [38].

The experimental data show that temperature greatly contributed to affecting the foaming events. A higher temperature affected the bubble drag, bubble rise velocity, surface tension, and flow behavior of the foam, which led to an increased mixing and gaseous hold up within the bubbles. These results are in accordance with a previous study [18]. The foam film permeability increased with the increasing temperature, whereas the surface tension decreased, as reported previously [39]. Temperature behaves as an indirect contributor to foaming events in photo-bioreactors. In Figure 8a,b, it is shown that foaming characteristics increased during the culture, such as FS from 0 to 9 s, FC from

0.28 ± 0.03 to 0.89 ± 0.03, and FE from 26 ± 0.41 to 38 ± 0.41. On the other hand, only FMD decreased from 6.1 ± 0.28 to 3.0 × 10^{-2} ± 0.28 (Figure 8b). The decreased FMD could be due to the fact that a higher temperature resulted in the formation of larger but less dense bubbles, which caused rapid drainage of liquid through the film-forming unstable foam.

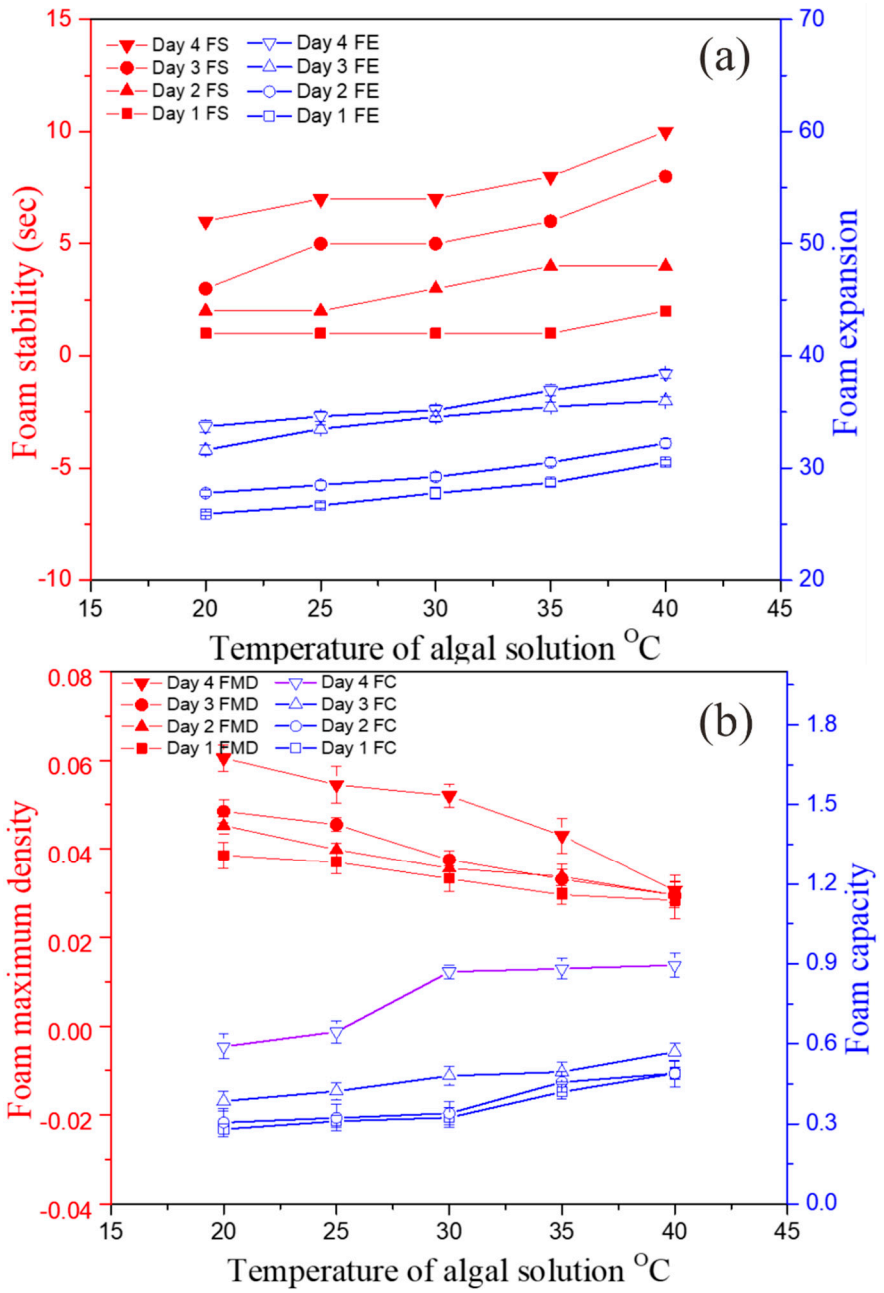

Figure 8. Effects of temperatures on dynamic characteristics: (**a**) foam stability and expansion and (**b**) foam maximum density and capacity.

4. Conclusions

The foaming mechanism in algal culture was investigated with varying CO_2 flow rates and temperature using a Foamscan instrument. It is concluded that, as the microalgae solution became denser and reached 2.4 g/L, the adhesive EPS released from *A. platensis* decreased the surface tension to 45 mN/m. Consequently, an increased CO_2 flow rate of 400 mL/min and a temperature of 40 °C increased the stability of the foam up to 10 s with 30 mm height and 1.8 mm bubble diameter. Based on the findings of this study, it is

recommended that a high temperature and rigorous CO_2 aeration should be avoided to mitigate the foaming problem in photobioreactors.

Author Contributions: Conceptualization, A.A.K., A.A., M.W.U. and J.C; methodology, A.A.K. and A.A; software, A.A.K. and S.K.; validation, A.A.K. and K.F.S.A.; formal analysis, A.A.K. and S.K.; investigation, A.A.K. and A.A.; resources, M.W.U. and J.C.; data curation, A.A.K., A.A. and K.F.S.A.; writing—original draft preparation, A.A.K., A.A. and M.W.U.; writing—review and editing, M.W.U., S.H., M.I. and J.C.; visualization, A.A.K.; supervision, M.W.U. and J.C.; project administration, M.W.U. and J.C.; funding acquisition, J.C. All authors have read and agreed to the published version of the manuscript.

Funding: This study was financially supported by the National Key Research and Development Program of China (2017YFE0122800), Zhejiang Provincial Key Research and Development Program of China (2020C04006), National Natural Science Foundation of China (21978120), Key R&D projects in Jiangsu Province (BE2020405), the Natural Science Foundation of Jiangsu Province (BK20200889), the Chinese Postdoctoral Science Foundation (2019M661761), and the Natural Science Foundation of Jiangsu Higher Education Institutions (20KJB550003).

Institutional Review Board Statement: Not applicable.

Informed Consent Statement: Not applicable.

Data Availability Statement: Not applicable.

Acknowledgments: The researchers are thankful to the analysis and testing centers of Jiangsu University, Zhenjiang, China, and Zhejiang University, Hangzhou, China, for the characterization of different samples.

Conflicts of Interest: The authors declare no conflict of interest. The funders had no role in the design of the study; in the collection, analyses, or interpretation of data; in the writing of the manuscript, or in the decision to publish the results.

References

1. Zhao, B.; Su, Y.; Zhang, Y.; Cui, G. Carbon Dioxide Fi Xation and Biomass Production from Combustion Fl Ue Gas Using Energy Microalgae. *Energy* **2015**, *89*, 347–357. [CrossRef]
2. Ganesh Saratale, R.; Kumar, G.; Banu, R.; Xia, A.; Periyasamy, S.; Dattatraya Saratale, G. A Critical Review on Anaerobic Digestion of Microalgae and Macroalgae and Co-Digestion of Biomass for Enhanced Methane Generation. *Bioresour. Technol.* **2018**, *262*, 319–332. [CrossRef] [PubMed]
3. Reen, S.; Chyuan, H.; Wayne, K.; Loke, P.; Phang, S.; Chuan, T.; Nagarajan, D.; Lee, D. Sustainable Approaches for Algae Utilisation in Bioenergy Production. *Renew. Energy* **2017**, *129*, 838–852. [CrossRef]
4. Ho, S.; Chen, C.; Lee, D.; Chang, J. Perspectives on Microalgal CO 2 -Emission Mitigation Systems—A Review. *Biotechnol. Adv.* **2011**, *29*, 189–198. [CrossRef] [PubMed]
5. Razzak, S.A.; Hossain, M.M.; Lucky, R.A.; Bassi, A.S.; Lasa, H. De Integrated CO 2 Capture, Wastewater Treatment and Biofuel Production by Microalgae Culturing—A Review. *Renew. Sustain. Energy Rev.* **2013**, *27*, 622–653. [CrossRef]
6. Khan, S.; Siddique, R.; Huanfei, D.; Shereen, M.A.; Nabi, G.; Bai, Q.; Manan, S.; Xue, M.; Ullah, M.W.; Bowen, H. Perspective Applications and Associated Challenges of Using Nanocellulose in Treating Bone-Related Diseases. *Front. Bioeng. Biotechnol.* **2021**, *9*, 350. [CrossRef] [PubMed]
7. Ullah, M.W.; Manan, S.; Kiprono, S.J.; Ul-Islam, M.; Yang, G. Synthesis, Structure, and Properties of Bacterial Cellulose. In *Nanocellulose: From Fundamental to Advanced Materials*; Huang, J., Lin, N., Dufresne, A., Eds.; Wiley: Weinheim, Germany, 2019; pp. 81–113. [CrossRef]
8. Pires, J.C.M.; Alvim-ferraz, M.C.M.; Martins, F.G. Photobioreactor Design for Microalgae Production through Computational Fl Uid Dynamics: A Review. *Renew. Sustain. Energy Rev.* **2017**, *79*, 248–254. [CrossRef]
9. Lee, E.; Pruvost, J.; He, X.; Munipalli, R.; Pilon, L. Design Tool and Guidelines for Outdoor Photobioreactors. *Chem. Eng. Sci.* **2014**, *106*, 18–29. [CrossRef]
10. Spolaore, P.; Joannis-Cassan, C.; Duran, E.; Isambert, A. Commercial Applications of Microalgae. *J. Biosci. Bioeng.* **2006**, *101*, 87–96. [CrossRef] [PubMed]
11. Prussi, M.; Buffi, M.; Casini, D.; Chiaramonti, D.; Martelli, F.; Carnevale, M.; Tredici, M.R. ScienceDirect Experimental and Numerical Investigations of Mixing in Raceway Ponds for Algae Cultivation. *Biomass Bioenergy* **2014**, *67*, 390–400. [CrossRef]
12. Pankratz, S.; Oyedun, A.O.; Zhang, X.; Kumar, A. Algae Production Platforms for Canada ' s Northern Climate. *Renew. Sustain. Energy Rev.* **2017**, *80*, 109–120. [CrossRef]

13. de Godos, I.; Mendoza, J.L.; Acién, F.G.; Molina, E.; Banks, C.J.; Heaven, S.; Rogalla, F. Evaluation of Carbon Dioxide Mass Transfer in Raceway Reactors for Microalgae Culture Using Flue Gases. *Bioresour. Technol.* **2014**, *153*, 307–314. [CrossRef] [PubMed]
14. Wang, J.; Nguyen, A.V.; Farrokhpay, S. A Critical Review of the Growth, Drainage and Collapse of Foams. *Adv. Colloid Interface Sci.* **2016**, *228*, 55–70. [CrossRef] [PubMed]
15. Chen, X.W.; Yang, D.X.; Zou, Y.; Yang, X.Q. Stabilization and Functionalization of Aqueous Foams by Quillaja Saponin-Coated Nanodroplets. *Food Res. Int.* **2017**, *99*, 679–687. [CrossRef] [PubMed]
16. Xu, L.; Xu, G.; Gong, H.; Dong, M.; Li, Y.; Zhou, Y. Colloids and Surfaces A: Physicochemical and Engineering Aspects Foam Properties and Stabilizing Mechanism of Sodium Fatty Alcohol Polyoxyethylene Ether Sulfate-Welan Gum Composite Systems. *Colloids Surfaces A Physicochem. Eng. Asp.* **2014**, *456*, 176–183. [CrossRef]
17. Kougias, P.G.; Boe, K.; Tsapekos, P.; Angelidaki, I. Bioresource Technology Foam Suppression in Overloaded Manure-Based Biogas Reactors Using Antifoaming Agents. *Bioresour. Technol.* **2014**, *153*, 198–205. [CrossRef]
18. Subramanian, B.; Pagilla, K.R. Colloids and Surfaces B: Biointerfaces Mechanisms of Foam Formation in Anaerobic Digesters. *Colloids Surfaces B Biointerfaces* **2015**, *126*, 621–630. [CrossRef]
19. Kougias, P.G.; Boe, K.; Einarsdottir, E.S.; Angelidaki, I. ScienceDirect Counteracting Foaming Caused by Lipids or Proteins in Biogas Reactors Using Rapeseed Oil or Oleic Acid as Antifoaming Agents. *Water Res.* **2015**, *79*, 119–127. [CrossRef]
20. Moeller, L.; Lehnig, M.; Schenk, J.; Zehnsdorf, A. Bioresource Technology Foam Formation in Biogas Plants Caused by Anaerobic Digestion of Sugar Beet. *Bioresour. Technol.* **2015**, *178*, 270–277. [CrossRef]
21. Kubar, A.A.; Cheng, J.; Kumar, S.; Liu, S.; Chen, S.; Tian, J. Strengthening Mass Transfer with the Tesla-Valve Baffles to Increase the Biomass Yield of Arthrospira Platensis in a Column Photobioreactor. *Bioresour. Technol.* **2021**, *320*, 124337. [CrossRef]
22. Cheng, J.; Guo, W.; Song, Y.; Kumar, S.; Ameer Ali, K.; Zhou, J. Enhancing Vorticity Magnitude of Turbulent Flow to Promote Photochemical Efficiency and Trichome Helix Pitch of Arthrospira Platensis in a Raceway Pond with Conic Baffles. *Bioresour. Technol.* **2018**, *269*, 1–8. [CrossRef] [PubMed]
23. Ali Kubar, A.; Cheng, J.; Guo, W.; Kumar, S.; Song, Y. Development of a Single Helical Baffle to Increase CO_2 Gas and Microalgal Solution Mixing and Chlorella PY-ZU1 Biomass Yield. *Bioresour. Technol.* **2020**, *307*, 123253. [CrossRef] [PubMed]
24. Kumar, S.; Cheng, J.; Guo, W.; Ali, K.A.; Song, Y. Self-Rotary Propellers with Clockwise/Counterclockwise Blades Create Spiral Flow Fields to Improve Mass Transfer and Promote Microalgae Growth. *Bioresour. Technol.* **2019**, *286*, 121384. [CrossRef] [PubMed]
25. Jones, S.A.; Laskaris, G.; Vincent-Bonnieu, S.; Farajzadeh, R.; Rossen, W.R. Effect of Surfactant Concentration on Foam: From Coreflood Experiments to Implicit-Texture Foam-Model Parameters. *J. Ind. Eng. Chem.* **2016**, *37*, 268–276. [CrossRef]
26. Wang, H.; Guo, W.; Zheng, C.; Wang, D.; Zhan, H. Effect of Temperature on Foaming Ability and Foam Stability of Typical Surfactants Used for Foaming Agent. *J. Surfactants Deterg.* **2017**, *20*, 615–622. [CrossRef]
27. Trabelsi, L.; M'sakni, N.H.; Ouada, H.B.; Bacha, H.; Roudesli, S. Partial Characterization of Extracellular Polysaccharides Produced by Cyanobacterium Arthrospira Platensis. *Biotechnol. Bioprocess Eng.* **2009**, *14*, 27–31. [CrossRef]
28. Chentir, I.; Hamdi, M.; Doumandji, A.; HadjSadok, A.; Ouada, H.B.; Nasri, M.; Jridi, M. Enhancement of Extracellular Polymeric Substances (EPS) Production in Spirulina (Arthrospira Sp.) by Two-Step Cultivation Process and Partial Characterization of Their Polysaccharidic Moiety. *Int. J. Biol. Macromol.* **2017**, *105*, 1412–1420. [CrossRef]
29. Liu, Q.; Zhang, S.; Sun, D.; Xu, J. Foams Stabilized by Laponite Nanoparticles and Alkylammonium Bromides with Different Alkyl Chain Lengths. *Colloids Surfaces A Physicochem. Eng. Asp.* **2010**, *355*, 151–157. [CrossRef]
30. Georgieva, D.; Cagna, A.; Langevin, D. Link between Surface Elasticity and Foam Stability. *Soft Matter* **2009**, *5*, 2063–2071. [CrossRef]
31. Saint-Jalmes, A. Physical Chemistry in Foam Drainage and Coarsening. *Soft Matter* **2006**, *2*, 836. [CrossRef]
32. Roth, A.E.; Jones, C.D.; Durian, D.J. Bubble Statistics and Coarsening Dynamics for Quasi-Two-Dimensional Foams with Increasing Liquid Content. *Phys. Rev. E-Stat. Nonlinear Soft Matter Phys.* **2013**, *87*, 1–14. [CrossRef] [PubMed]
33. Bernaerts, T.M.M.; Gheysen, L.; Foubert, I.; Hendrickx, M.E.; Van Loey, A.M. The Potential of Microalgae and Their Biopolymers as Structuring Ingredients in Food: A Review. *Biotechnol. Adv.* **2019**, *37*, 107419. [CrossRef] [PubMed]
34. Singh, S.P.; Singh, P. Effect of Temperature and Light on the Growth of Algae Species: A Review. *Renew. Sustain. Energy Rev.* **2015**, *50*, 431–444. [CrossRef]
35. Ahmed, M.; Moerdijk-Poortvliet, T.C.W.; Wijnholds, A.; Stal, L.J.; Hasnain, S. Isolation, Characterization and Localization of Extracellular Polymeric Substances from the Cyanobacterium Arthrospira Platensis Strain MMG-9. *Eur. J. Phycol.* **2014**, *49*, 143–150. [CrossRef]
36. Renaud, S.M.; Thinh, L.-V.; Lambrinidis, G.; Parry, D.L. Effect of Temperature on Growth, Chemical Composition and Fatty Acid Composition of Tropical Australian Microalgae Grown in Batch Cultures. *Aquaculture* **2002**, *211*, 195–214. [CrossRef]
37. Mancuso Nichols, C.A.; Nairn, K.M.; Glattauer, V.; Blackburn, S.I.; Ramshaw, J.A.M.; Graham, L.D. Screening Microalgal Cultures in Search of Microbial Exopolysaccharides with Potential as Adhesives. *J. Adhes.* **2009**, *85*, 97–125. [CrossRef]
38. Muñoz, R.; Guieysse, B. Algal-Bacterial Processes for the Treatment of Hazardous Contaminants: A Review. *Water Res.* **2006**, *40*, 2799–2815. [CrossRef]
39. Kapetas, L.; Vincent Bonnieu, S.; Danelis, S.; Rossen, W.R.; Farajzadeh, R.; Eftekhari, A.A.; Mohd Shafian, S.R.; Kamarul Bahrim, R.Z. Effect of Temperature on Foam Flow in Porous Media. *J. Ind. Eng. Chem.* **2016**, *36*, 229–237. [CrossRef]